CHEMICAL ENGINEERING TRANSACTIONS
VOL. 33, 2013
Guest Editors: Enrico Zio, Piero Baraldi

ISBN 978-88-95608-24-2; **ISSN** 1974-9791

A publication of
AIDIC
The Italian Association
of Chemical Engineering
Online at: www.aidic.it/cet

DOI: 10.3303/CET1333184

Geometrical and Dimensional Uncertainties Effects Quantification for Stress/Strain Field Characterization

Gabriele Marcuccio*[a], John Mottershead[b], Elvio Bonisoli[a], Stefano Tornincasa[a], Edoardo Patelli[c]

[a]Department of Management and Production Engineering – Politecnico di Torino, Corso Duca degli Abruzzi 24, 10129, Torino, Italia
[b]Centre for Engineering Dynamics, School of Engineering – University of Liverpool, Harrison Hughes Building, L69 3GH, Liverpool, UK
[c]Institute for risk and uncertainty, School of Engineering – University of Liverpool, Brodie Tower L69 3GQ, Liverpool, UK
gabriele.marcuccio@polito.it

In the automotive industry a significant part of research is dedicated to design and produce better products. The unavoidable presence of uncertainties in manufacturing processes and structural parameters leads to the necessity to develop stochastic models able to correctly represent physical behaviours. This paper presents numerical and experimental investigations on the effects of the fitting process on the stress/strain map of assembled automotive rim-disk systems. Different strategies of geometrical decomposition are used to condense large volumes of data by retaining essential information for the whole design process including not only manufacturing pre-stresses and operational loads but also dimensional tolerances of mating parts by means of a probabilistic model. Efficient approaches are used to identify the relative importance of input factors on the output uncertainties. A real test case of a wheel assembly is presented and discussed.

1. Introduction

Since the end of the last century the automotive industry has required cost-sensitive and energy-efficient products. The demand of lightweight components has grown again due to the rising importance of low emissions vehicles and the large scale production of electric cars. Nowadays, a significant part of research is dedicated to the identification and control of characteristics and performance factors needed to improve in product design (Saltelli et al., 2008). The automotive wheel field is an example of active area on design and development of new components that must respect styling limits, durability performance (e.g. $3*10^5$ km for cars, and $5*10^5$ km for trucks), weight constraints, manufacturing costs and noise-vibration-harshness targets. Since tyres and wheels are recognised as making one of the major contribution to road safety, the European Tires and Rim Technical Organization (ETRTO) promotes the establishment of common engineering dimensions, pressure and loads characteristic and operational guidelines, aimed to make appropriate recommendations and align national and international standards without disregarding safety aspects. All standardized tests wheel manufacturers must comply with (Official Journal of the European Union, 2006, ETRTO Standard Manual 2012) aim to reduce the parameters under control in order to increase the repeatability of experiments performed and make the trials more reliable and accurate. Usually only few output variables namely, fatigue life in terms of number of cycles, maximum stress, or stiffness values (radial or axial) are considered. Nevertheless, numerical analyses by means of finite element models (FEM) are able to predict and to identify critical regions in the early design phase (see e.g. Kocabicak and Firat (2001), Wang and Zhang (2010), Firat et al. (2009)). The final size of a manufactured component depends on the quality and precision of the process and in spite of precise machining there will always be a deviation from nominal size. Technical drawings and real parts can differ slightly, making hard for the analysts to understand if those deviations can be seen as responsible factors to durability drops and performance reductions. This happens not only because operating conditions, most

of the time, cannot be kept under control but also as manufacturing processes give rise to uncertainties related to both dimensional and geometric tolerances. The presence of even small technological or metallurgical defects (Carboni et al., 2003), process variability and deficiency (Grath et al., 2000), variation in material ratios, or even surface texture typology can noticeably influence the stress-strain map and prevent from making flawless wheels. Although large uncertainties are associated with structural parameters, their effects on the component behaviour are often either neglected or not considered.
In this paper, numerical and experimental investigations on the effects of the fitting process on the stress/strain map of assembled automotive components, namely steel wheels, are reported. Full field decomposition through orthogonal kernel functions are used to condense large volumes of data by retaining essential information (Wang et al., 2012) for the whole design process, from technical drawing to experimental validation, taking into account not only manufacturing pre-stresses but also dimensional tolerances of mating parts by means of a probabilistic model. The effect of uncertainty have been quantified by means of a general purpose software COSSAN-X (Patelli et al., 2012). A screening of the most important parameters is performed with time and computational costs that are compatible with industry and production constraints.

2. Numerical model

The component analysed is a steel wheel composed by a rim and a disc. The disc is made of a material equivalent to DP600, whereas the rim is FEP11. The material properties for the elements above are as follow: Young's modulus E= 210 GPa, Poisson ratio ν =0.3, density ρ = 7900 kg/m^3. All the degrees of freedom of the outer flange rim are constrained, and by applying symmetry boundary conditions only a portion (1/4) of the system is analysed.

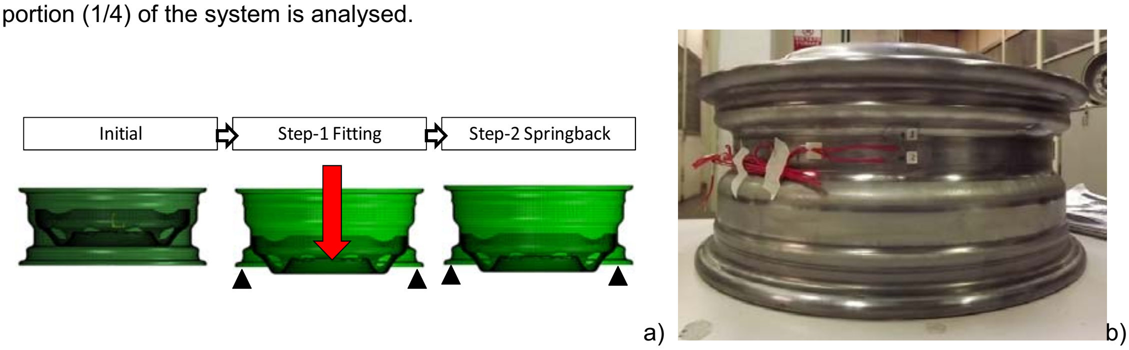

Figure 1: Simulation steps and boundary conditions (left), final wheel assembly (right)

The procedure is divided into two steps that simulate the fitting process and the following spring-back phase (Figure 1). Elasto-plastic material with an isotropic hardening formulation is used. The model is solved and the Von Mises stresses around venting holes, where in experimental tests crack usually nucleates and propagates, and close to the rim wells, where the disc and rim are welded, are shown in Figure 2. Despite the simulation describes only the fitting process, some of the most critical areas reported in Carboni et al. (2003), and Kocabicak and Firat (2001) are already depicted (Figure 2). At manufacturing stage, hot rolled units, i.e. metal coils, need to fulfil mechanical properties in an acceptability range.

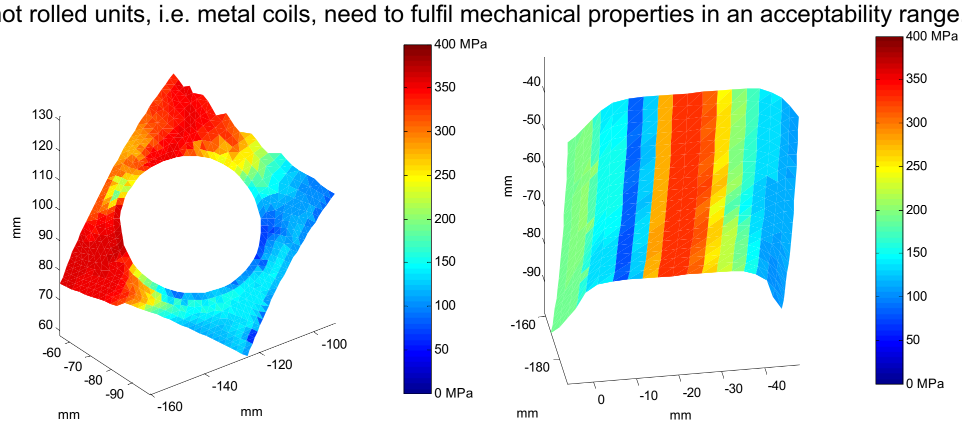

Figure 2: Full-field stress data: around venting hole (left), near rim well (right)

Target values, upper and lower bounds are defined for each lot. The steel wheel is modelled in Abaqus Standard/Explicit using shell elements (CQUAD4 and CTRIA3) whose dimensions are 2mm in average. The uncertainty in the geometry and material properties has been modelled by means of 12 random variables uniformly distributed, representing the admissible tolerance (Table1).

Table 1: Design of experiments set up: geometrical and material affecting factors

Factor number	Factor name	Factor number	Factor name
1	Young modulus E	7	DP600 thickness
2	Yield point (DP600)	8	FEP11 thickness
3	Plastic stiffness (DP600)	9	Diameter disc
4	Yield point (FEP11)	10	Diameter rim
5	Plastic stiffness (FEP11)	11	Scallop depth
6	Friction coefficient	12	Flange angle

Yield point (Yp), ultimate tensile strength (UTS) and corresponding strain were chosen for defining some of the characteristic points needed during the simulation in the elasto-plastic region. The screening method (one-factor-a-time" experiments) provides a simple and rapid approach to perform global sensitivity analysis. This approach does not allow to investigate the interaction among factors, but gives a rough idea on how each input factor can affect the quantity of interest (i.e. the fitting force behaviour). The regions defined by the upper and lower bounds of each varying factors are shown in Figure 3. It would be impossible to control all the investigated parameters and to reproduce experimentally the same conditions.

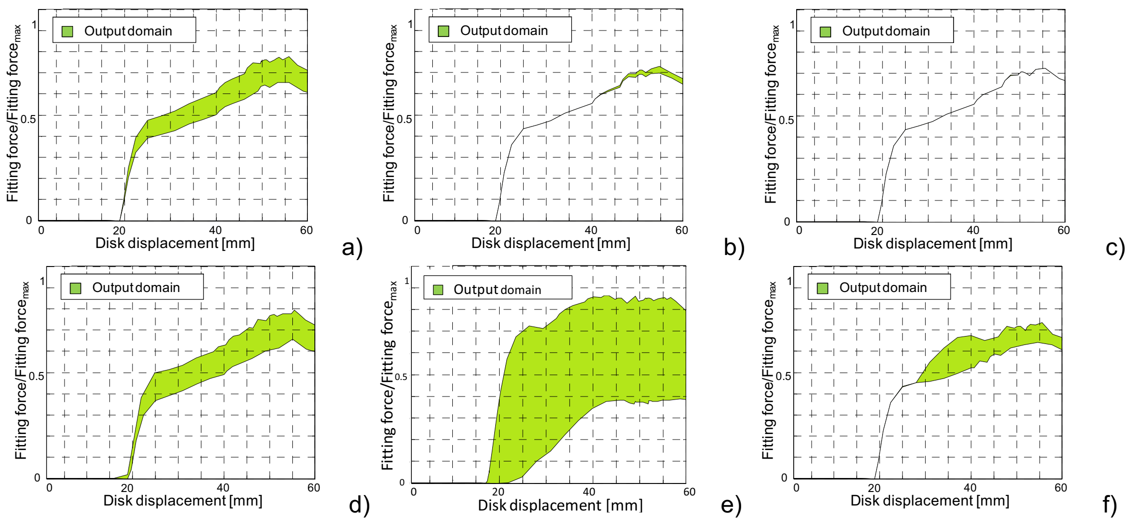

Figure 3: Effect of input factor on fitting force curve: a) factor 1, b) factor 2, c) factor 3, d) factor 8, e) factor 9, f) factor 12

3. Experiment and model validation

The experimental strain analysis has been adopted to validate the numerical analysis. A couple of disc and rim was taken from the production batch and deeply measured. Components satisfied the design and ETRTO profile requirements. Leadwire equipped gauges were bonded with cyanoacrylate adhesive to the metal sheet surface of the specimens, as shown in Figure 1, and the fitting process was performed. All the strains and the applied force, necessary to fit the disc inside the rim, were measured and recorded during the press-fit, by means of a load cell and an acquisition system (Figure 4). The experimental fitting force shows a highly non-linear behaviour due to the difficulty in keeping a low and constant press speed. The oscillations after the first ramp up phase are due axial adjustments of the disk with respect to the rim and to the presence of stick-slip phenomena, neglected during the numerical simulation. The experimental results have been compared with 500 numerical analyses. Latin hypercube sampling strategy has been adopted to explore the input space, with the *maximin* metric introduced by Johnson et al. (1990). Because of the need to maintain a reasonable computational time, the sample plan size was reduced to the least possible without losing reliability of solutions. Results show a good agreement between the numerical model and the experimental test. Both the fitting force curve and strain curve lay into the response region

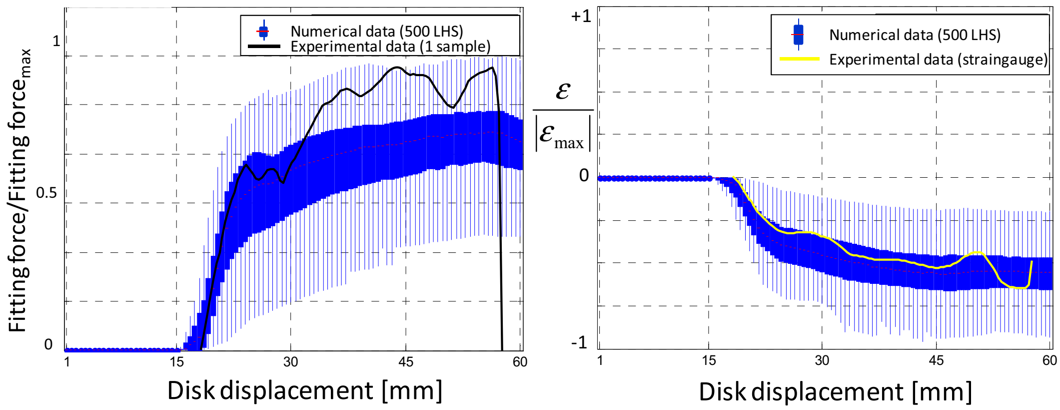

Figure 4: Fitting force behaviour and strain trend (SG1): numerical and experimental comparison

covered by numerical data, pointing out a first steep increase from the contact point to the first 15 mm of disc fitting. For each boxplot the central red mark corresponds to the median, the edge of the box are the 25-th and 75-th percentiles, the whiskers extend to the 99.3 % of the output data at that step. During the experiment the force applied to the disc was removed before reaching the nominal displacement target. By considering these output responses two main limits can be pinpointed: i) the applied force allows to describe the complete assembly and summarize the main effect of its variable input factors but do not give any idea on which are the main stressed areas, ii) measurements by means of straingauges can be misleading because they quantify just local deformations without giving information on wider regions from a more global point of view. However stress/strain data obtained from numerical simulations can overcame this issue if properly post-processed.

4. Geometric moments theory

Two-dimensional moment invariants were initially introduced to recognise plane patterns, to process visual information and to efficiently recapture all the image features in a reduced and compact sequence of real numbers. The adaptive geometric moment descriptor as proposed by Wang et al. (2012) was adopted. For the analysis of the wheel are defined as,

$$S_r = \int_{\Omega} w(\mathbf{x}(u,v)) \frac{1}{\sqrt{\mu}} G_r(u,v) \left\| \frac{\partial \mathbf{x}}{\partial u} \times \frac{\partial \mathbf{x}}{\partial v} \right\| du\, dv \cong \sum_{k}^{All\ nodes} w(\mathbf{x}(u_k,v_k)) G_r(u_k,v_k) \sqrt{\Delta_s^k \Delta_{uv}^k} \qquad (1)$$

where $w(\mathbf{x}(u_k,v_k))$ are the full-field data, $G_r(u_k,v_k)$ represents the kernel functions, Δ_s^k is the area of the k-th element in 3D surface, Δ_{uv}^k is the area of the k-th element in 2D parametric space. Two dimensional monomials were used as kernel functions, expressed as,

$$G_o(u_k,v_k) = G_{p,q}(u_k,v_k) = u^p v^q \qquad (2)$$

Where *u, v* ∈ ℝ and *p, q* ∈ ℕ. It was necessary to apply the Modified Gram Schmidt orthogonalisation (MGSO) instead of the classical approach (CGSO) to achieve the orthogonality of monomials when high orders of the kernel functions are implemented. Orthogonal kernel functions require simple and regular domains, but both disc and rim, as many others engineering structures have a complex, irregular and non-flat surface. A surface mapping Ψ between a mesh *M* and an isomorphic planar triangulation *U* is required. The 3D position of the i^{th} node is denoted by $\mathbf{x}_i=(x_i,y_i,z_i)$, while the corresponding position of the node on the 2D domain by $\mathbf{u}_i=(u_i,v_i)$. Surface mapping is therefore providing the transformation that links the 3D domain to the planar domain, such as:

$$\Psi : M \in R^3 \rightarrow U \in R^2,\ x_i(x_i,y_i,z_i) \rightarrow u_i(u_i,v_i) \qquad (3)$$

Since the choice among the techniques (isometric, harmonic, conformal, authalic, and nonlinear map) proposed for minimising the distortion of the elements over a linear surface seems very arbitrary (Desbrun and Meyers, 2002, Floater and Hormann, 2005), a mapping that inversely simulates the process of metal sheet forming is used. First, the profile of the disc is lengthened, then the 3D surface is flattened while preserving the total area. Even if the transformation is not properly authalic the total area ratio is kept constant and the new mesh is still regular, with an average element size of 2 mm (Table 3). Analogous transformation is applied to the rim. The Adaptive Geometric Moment Descriptor (AGMD) of the stress field (Von Mises criteria) near the venting hole and for the rim well region are shown in Figure 5. A small number (20-30) of the most significant features are sufficient to approximate and reconstruct the complete stress field. The orders of the kernel functions are respectively $n \in [0,1,...,6]$, $m \in [0,1,...,6]$ (left), and $n \in [0,1,...,5]$ and $m \in [0,1,...,17]$ (right).

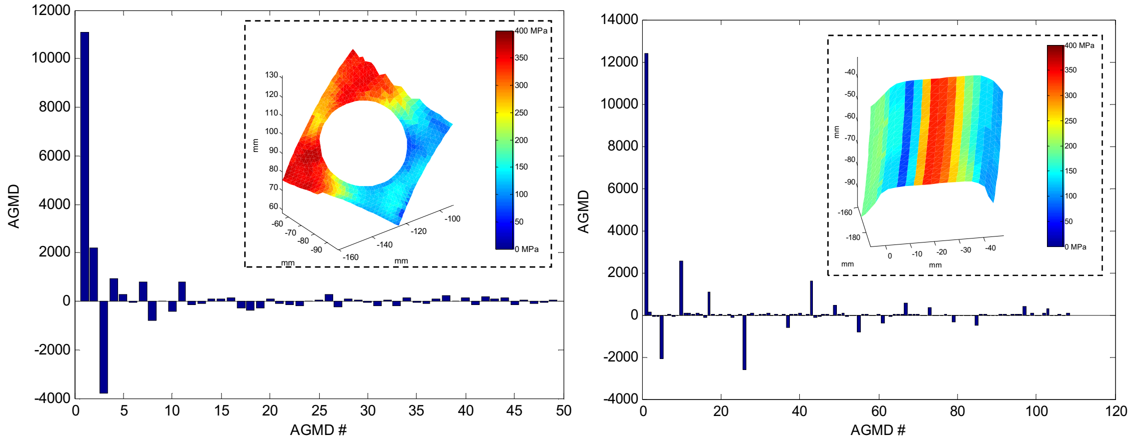

Figure 5: Adaptive geometric moment descriptors and reconstructed stress field from AGMD of venting hole region (left) and rim well region (right)

5. Product variability quantification

The optimal design procedure of components that need to resist to static loads or fatigue constraints is widely based on iterative change of the design variables that are mainly responsible of the peak of stresses in the most critic regions. By evaluating only the maximum values of equivalent stress, information related to the position or the changes of the map of stress on a more wide region is lost. Moment descriptors can overcome this problem condensing large volume of data and retaining the essential information, at least 90-95% of the original set, in order to reconstruct full fields from a simple array of real numbers. In a LHS plan if few parameters are changed at the same time, the full-field of measured data can greatly differ over the input domain region. For the numerical test case proposed, an evaluation of the variability of the first 20 moment descriptors is given (Figure 6).

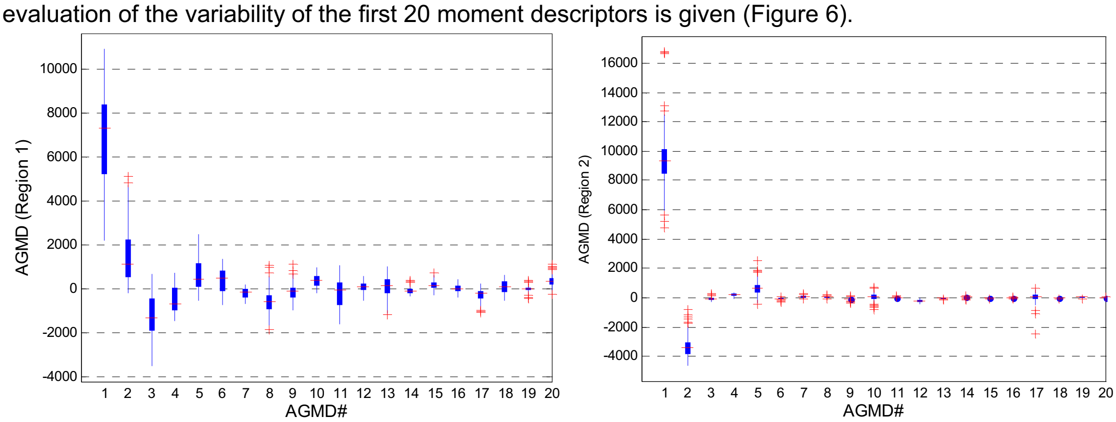

Figure 6: Adaptive geometric moment descriptor variability: region 1 (left), region 2 (right)

The 12 factors are varied in the whole input domain, and a great sensitivity of the AGMD is depicted (Figure 6, left). However only some of the moment descriptors related to region 2 (i.e. MD_1, MD_2, MD_3, MD_5, MD_{10}, MD_{17}) seem to be influenced by a change of the input parameters and a smaller variability is shown. By looking more in deep at the AGMD trend, when just one of the input parameter (factor 10) is changed, it is possible to identify a nonlinear relationship between each shape descriptor and the interference fit value (Figure 7). The interference fit value is mainly dependent on disc size, rim size, metal sheet thickness, and geometry, but if only one parameter is varied, the dependency shown is with the factor itself and becomes more evident. In general it is possible to establish a direct link between the uncertainty associated to a parameter with the variability of the output response. The method could be used for determining not only acting but also allowable stresses in critical sections of the wheel.

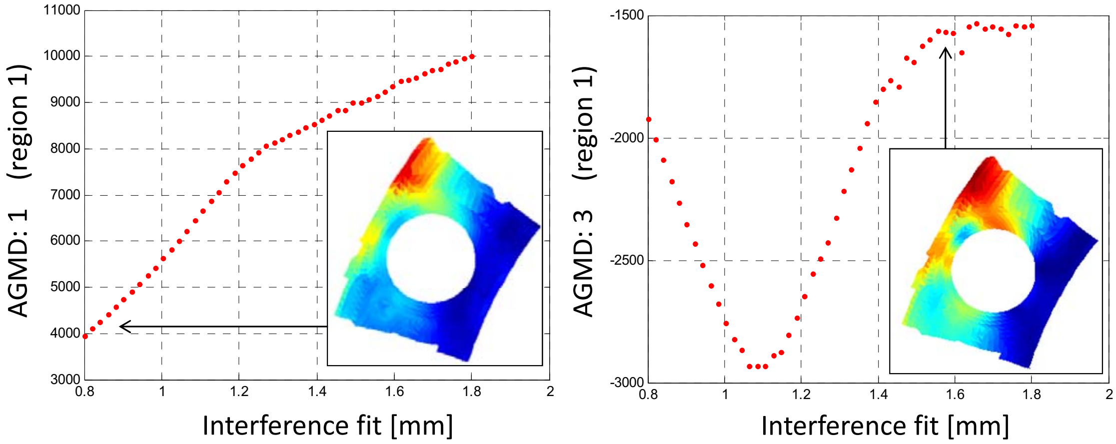

Figure 7: Adaptive geometric moment descriptor trends (50 samples): region 1

Conclusions

Numerical and experimental investigations on the effects of the fitting process on the stress/strain map of steel wheels have been shown. The performed numerical analysis on the presented assembly takes into account aspects usually neglected: manufacturing pre-stresses and dimensional tolerances of mating parts by means of a probabilistic model. Full field decomposition through orthogonal kernel functions are used to condense large volumes of data. Essential information of the stress map for those critical regions that could give rise to wheel failures, can be summarized in approximately 20 shape descriptors. A numerical-experimental correlation on fitting force behaviour is used as the starting point for identifying the most important factors. The ideas presented here are expected to prove valuable in uncertainty quantification problems, damage detection and meta-models development.

References

Carboni M., Beretta S., Finzi A., 2003, Defects in-sevice fatigue life of truck wheels, Engineering Failure Analysis, 10, 45-57.

Desbrun M., Meyer M., Alliez P., 2002, Intrinsic parameterizations of surface meshes, Computer graphics forum, 21.

Firat M., Kozan R., Ozsoy M., Mete O.M., 2009, Numerical modelling and simulation of wheel radial fatigue tests, Engineering Failure Analysis, 16, 1533-1541.

Floater M., Hormann K., 2005, Surface parameterization: a tutorial and survey, Advances in Multiresolution for Geometric Modelling, 157-186.

Grath P.J., Hatting D.G., James M.N., Els-Botes A., 2000, Effects of forming process on fatigue performance of wheel centre discs. Proceedings ECF13, San Sebastian.

Johnson M.E., Moore L.M., Ylvisaker D., 1990, Minimax and maximin distance designs, Journal of statistical Planning and Inference, 26, 131-148.

Kocabicak U., Firat M., 2001, Numerical analysis of wheel cornering fatigue tests, Engineering Failure Analysis, 8, 339-354.

Patelli E., Panayirci H., Broggi M., Goller B., Beaurepaire P., Pradlwarter H., Schuëller G., 2012, General purpose software for efficient uncertainty management of large finite element models, Finite Elements in Analysis and Design 51, 31–48.

Saltelli A., Ratto M., Andres T., Campolongo F., Cariboni J., Gatelli D., Saisana M., Tarantola S., Global sensitivity analyses: The Primer, 2008, John Wiley and Sons, New York, USA.

Wang X., Zhang X., 2010, Simulation of dynamic cornering fatigue test of a steel passenger car wheel, International Journal of Fatigue, 32, 434-442.

Wang W., Mottershead J.E., Siebert T., Pipino A., 2012, Frequency response functions of shape features from full-field vibration measurements using digital image correlation, Mechanical systems and signal processing, 28, 333-347.